

# HADRON-QUARK CROSSOVER AND MASSIVE HYBRID STARS WITH STRANGENESS

KOTA MASUDA

Department of Physics, The University of Tokyo, Tokyo 113-0033, Japan

TETSUO HATSUDA

Theoretical Research Division, Nishina Center, RIKEN, Wako 351-0198, Japan  
IPMU, The University of Tokyo, Kashiwa 277-8583, Japan

TATSUYUKI TAKATSUKA

Iwate University, Morioka 020-8550, Japan  
*Submitted to ApJ*

## ABSTRACT

Using the idea of smooth crossover from the hadronic matter with hyperons to quark matter with strangeness, we show that the maximum mass ( $M_{\max}$ ) of neutron stars with quark matter core can be larger than those without quark matter core. This is in contrast to the conventional softening of equation of state due to exotic components at high density. Essential conditions to reach our conclusion are (i) the crossover takes place at relatively low densities, around 3 times the normal nuclear density, and (ii) the quark matter is strongly interacting in the crossover region. By these, the pressure of the system can be greater than that of purely hadronic matter at a given baryon density in the crossover density region and leads to  $M_{\max}$  greater than 2 solar mass. This conclusion is insensitive to the different choice of the hadronic equation of state with hyperons. Several implications of this result to the nuclear incompressibility, the hyperon mixing, and the neutrino cooling are also remarked.

*Subject headings:* dense matter, elementary particles, equation of state, stars: neutron

## 1. INTRODUCTION

Since neutron stars (NSs) are gravitationally bound, observation of the NS mass ( $M$ ) provides a precious probe for the equation of state (EOS) and the relevant composition and structure of dense matter. The larger  $M$  requires a stiffer EOS and thereby gives a stringent condition on the state of matter, since various new phases proposed so far, such as pion condensation, kaon condensation, hyperon ( $Y$ ) mixing, deconfined quark matter and so on, are believed to soften the EOS.

For example, the EOS is softened dramatically when  $Y$  takes part in NS cores and the theoretical maximum mass fails to exceed the observed mass,  $M_{\text{obs}} = 1.44M_{\odot}$  for PSR1913+16 with  $M_{\odot}$  being the solar mass. This contradiction between theory and observation may indicate a missing repulsion in hyperonic matter such as the 3-body interaction (TNI) acting universally in the nucleon and hyperon sectors (Nishizaki et al. (2001); Takatsuka et al. (2006, 2008)).

Very recently, the observation of heavy NS with  $M = (1.97 \pm 0.04)M_{\odot}$  for PSR J1614-2230 (Demorest et al. (2010)) has been reported, which causes even stronger constraint on the EOS. In particular, it stimulates intensive discussions on whether such a heavy NS can have exotic components in the central core (Özel et al. (2010); Kurkela et al. (2010); Kim et al. (2011); Klahn et al. (2011); Lattimer et al. (2010); Weissenborn et al. (2011); Bonanno et al. (2012); Chen et al. (2012); Schramm et al. (2012); Whittenbury et al. (2012)).

In particular, in many of the previous works treating the transition from the hadron phase to the quark

phase at high density, point-like hadrons and quarks are treated as independent degrees of freedom, and Gibbs phase equilibrium conditions are imposed. However, quantum chromodynamics (QCD) tells us that such a description is not fully justified, since all hadrons are extended objects composed of quarks and gluons. Indeed, one may expect a gradual onset of quark degrees of freedom in dense matter associated with the percolation of finite-size hadrons, i.e., a smooth crossover from hadronic matter to quark matter: See seminal works on hadron percolation (Baym (1979); Celik et al. (1980)), recent works on hadron-quark crossover (Baym et al. (2008); Maeda et al. (2009)) and a recent review on phase transitions in dense QCD (Fukushima et al. (2011)).

The aim of this paper is to make a phenomenological study on the mechanism realizing hybrid stars (NS with a quark core) compatible with  $2M_{\odot}$  from the point of view of the smooth crossover between the hadronic matter with hyperons and the quark matter with strangeness. Unlike the traditional approach to the hadron-quark transition, the crossover picture gives us a novel tool to study whether the hybrid star with a quark core is compatible with massive neutron stars (Takatsuka et al. (2011)).

## 2. HADRONIC MATTER WITH STRANGENESS

Let us start with an example of hadronic EOS with hyperons (H-EOS) (Nishizaki et al. (2001, 2002); Takatsuka et al. (2006)) obtained with the following procedure: (i) Effective two-baryon potentials  $\tilde{V}_{BB'}$  ( $B = n, p, \Lambda, \Sigma^{-}$ ) are constructed on the basis of the G-matrix formalism to take into account their density-dependence. (ii) A phenomenological 3-body nucleon force  $\tilde{U}_{NN'}$  ex-

pressed in a form of two-body potential (Friedman et al. (1981)) is introduced to reproduce the saturation of symmetric nuclear matter (the saturation density  $\rho_0 = 0.17 \text{ fm}^{-3}$  and the binding energy  $E_0 = -16 \text{ MeV}$ ) and the incompressibility  $\kappa$ . (iii) We assume universal three-body repulsion even for the hyperons through the replacement,  $\tilde{U}_{NN'} \rightarrow \tilde{U}_{BB'}$ . (iv) By using  $\tilde{V}_{BB'} + \tilde{U}_{BB'}$ , we obtain the hadronic EOS under charge neutrality and  $\beta$ -equilibrium and calculate particle composition  $y_i$  ( $i = n, p, \Lambda, \Sigma^-, e^-$  and  $\mu^-$ ) as a function of total baryon density  $\rho$ . This gives our H-EOS of neutron star matter with hyperon mixing.

The stiffness of H-EOS is specified by  $\kappa$ ; the case with  $\kappa = 300$  (250) MeV is denoted by TNI3u (TNI2u). Here the subscript ‘‘u’’ means that the 3-body force is introduced universally including the hyperon sector. The maximum mass ( $M_{\text{max}}$ ) of the NSs with hyperon-mixed core with universal 3-body force becomes  $M_{\text{max}} \simeq 1.82(1.52)M_\odot$  for TNI3u (TNI2u): On the other hand, with only the nucleon 3-body force (TNI3), it reduces to  $M_{\text{max}} \simeq 1.1M_\odot$  which is not even compatible with  $M_{\text{obs}} = 1.44M_\odot$ . One of the effects of the universal 3-body force is to delay the onset of hyperon mixing, e.g.  $\rho_\Lambda \simeq \rho_{\Sigma^-} \simeq 4\rho_0$  for TNI3u and TNI2u cases, while  $\rho_{\Sigma^-} \simeq 2.2\rho_0$ ,  $\rho_\Lambda \simeq 2.5\rho_0$  for TNI3.

To check the model-dependence of the H-EOS, we consider two alternative equations of state with hyperons: AV18+TBF+ $\Lambda\Sigma$  (Baldo et al. (2000)) which is based on the G-matrix approach with the AV18 nucleon-nucleon potential, Urbana-type three-body nucleon potential and the Nijmegen soft-core nucleon-hyperon potential; SCL3 $\Lambda\Sigma$  (Tsubakihara et al. (2010)) which is a relativistic mean-field model with chiral SU(3) symmetry. The maximum masses (central baryon densities, radius) of NSs composed only by hadronic EOSs, AV18+TBF+ $\Lambda\Sigma$  and SCL3 $\Lambda\Sigma$ , are  $M_{\text{max}} \sim 1.22M_\odot$  ( $7.35\rho_0$ ,  $10.46\text{km}$ ) and  $M_{\text{max}} \sim 1.36M_\odot$  ( $5.89\rho_0$ ,  $11.42\text{km}$ ), respectively.

In Fig.1, we plot the energy per particle ( $E/A$ ) of hadronic EOS with hyperons (TNI3u, TNI2u, TNI3, and SCL3 $\Lambda\Sigma$ ) together with the nuclear EOS without hyperons, APR (Akmal et al. (1998)). We do not show AV18+TBF+ $\Lambda\Sigma$  since it is almost the same with TNI3. Filled circles on each line denote the density where the hyperons start to mix. From this figure, one can see that (i) the mixture of hyperons softens the equation of state relative to APR, and (ii) onset of the hyperon mixture is shifted to higher density if we consider the universal 3-body interaction. In the following, we adopt TNI3u as a typical example of the H-EOS and comment on the results with other H-EOSs at the end.

### 3. QUARK MATTER WITH STRANGENESS

Next we consider EOS of quark matter with strangeness (Q-EOS). Around the baryon density of a few times  $\rho_0$  where the hadron-quark crossover is expected to take place at zero temperature, the deconfined (or partially deconfined) quarks would be still strongly interacting. Analogous situation at high temperature has been expected theoretically and evidences of a strongly interacting quark-gluon plasma (sQGP) were found experimentally in relativistic heavy-ion collisions (see e.g. a review, Fukushima et al. (2011)).

Since numerical simulations of quantum chromodynamics (QCD) on the space-time lattice at high baryon

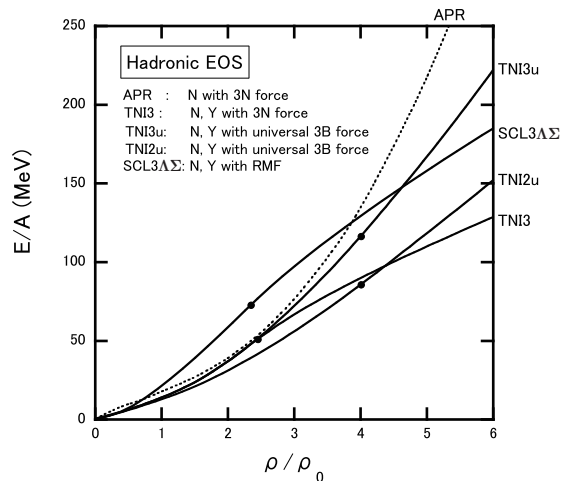


FIG. 1.— Energy per particle ( $E/A$ ) as a function of the total baryon density  $\rho$ . Solid lines denote EOSs with hyperon mixing; TNI3u (universal 3-baryon force with  $\kappa = 300\text{MeV}$ ), TNI3 (3-nucleon force with  $\kappa = 300\text{MeV}$ ), TNI2u (universal 3-baryon force with  $\kappa = 250\text{MeV}$ ), SCL3 $\Lambda\Sigma$  (relativistic mean-field model with chiral SU(3) symmetry). Dotted lines denote the EOS without hyperon, APR (AV18+ $\delta v$ + UIX\*). Filled circles on each line show the density where the hyperons start to mix.

density is not available due to the notorious sign problem, we treat the strongly interacting quark matter (sQM) at zero temperature by the (2+1)-flavor Nambu–Jona-Lasinio (NJL) model (see the reviews, (Vogel et al. (1991); Klevansky (1992); Hatsuda et al. (1994); Buballa (2005)). It is an effective theory of QCD and is particularly useful for taking into account the non-perturbative phenomena such as the partial restoration of chiral symmetry at high density. The model Lagrangian reads

$$\mathcal{L}_{\text{NJL}} = \bar{q}(i\cancel{\partial} - m)q + \frac{G_S}{2} \sum_{a=0}^8 [(\bar{q}\lambda^a q)^2 + (\bar{q}i\gamma_5\lambda^a q)^2] + G_D [\det \bar{q}(1 + \gamma_5)q + \text{h.c.}] - \frac{g_V}{2} (\bar{q}\gamma^\mu q)^2, \quad (1)$$

where the quark field  $q_i$  ( $i = u, d, s$ ) has three colors and three flavors with the current quark mass  $m_i$ . The term proportional to  $G_S$  is a  $U(3)_L \times U(3)_R$  symmetric four-fermi interaction where  $\lambda^a$  are the Gell-Mann matrices with  $\lambda^0 = \sqrt{2/3}I$ . The term proportional to  $G_D$  is the Kobayashi–Maskawa–’t Hooft (KMT) six-fermi interaction which breaks  $U(1)_A$  symmetry. The third term proportional to  $g_V$  is a phenomenological vector-type interaction. It has some varieties depending on its flavor-structure: Here we use the form given in Eq.(1) which leads to an universal flavor-independent repulsion among quarks.

In the mean-field approximation, the constituent quark masses  $M_i$  ( $i = u, d, s$ ) are generated dynamically through the NJL interactions ( $G_{S,D}$ ),  $M_i = m_i - 2G_S\sigma_i - 2G_D\sigma_j\sigma_k$ , where  $\sigma_i = \langle \bar{q}_i q_i \rangle$  is the quark condensate in each flavor, and  $(i, j, k)$  corresponds to the cyclic permutation of  $u, d$  and  $s$ . On the other hand, the vector interaction ( $g_V$ ) leads to an effective chemical potential (Asakawa et al. (1989)),  $\mu_i^{\text{(eff)}} = \mu_i - g_V \sum_j \langle q_j^\dagger q_j \rangle$ .

Basic parameters of the NJL model are determined from hadron phenomenology: In this paper, we adopt so-called the HK parameter set (Hatsuda et al. (1994)),  $\Lambda =$

631.4 MeV,  $G_S \Lambda^2 = 1.835$ ,  $G_D \Lambda^5 = 9.29$ ,  $m_{u,d} = 5.5$  MeV,  $m_s = 135.7$  MeV, where  $\Lambda$  is the three-momentum cutoff. The magnitude of  $g_v$  has not been well determined, but recent studies of the model applied to the QCD phase diagram suggest that it can be comparable to or even larger than  $G_S$  (Bratovic et al. (2012); Lourenco et al. (2012)), so that we change its value in the range,

$$0 \leq \frac{g_v}{G_S} \leq 1.5. \quad (2)$$

The EOS of strongly interacting quark matter with strangeness is obtained from the above model under charge neutrality and  $\beta$ -equilibrium with  $u$ ,  $d$ ,  $s$ ,  $e^-$  and  $\mu^-$ . It turns out that the strange quarks starts to appear at  $\rho \simeq 4\rho_0$  regardless of the magnitude of  $g_v$ . Also,  $\mu^-$  never appears under the presence of the strangeness.

#### 4. HADRON-QUARK CROSSOVER

To realize the smooth transition between the hadronic matter and the quark matter, we first define a ‘‘crossover density region’’ characterized by its central value  $\bar{\rho}$  and its width  $\Gamma$ . The description of the matter in terms of the pure hadronic EOS is accurate for  $\rho \ll \bar{\rho} - \Gamma$ , while the description in terms of pure quark EOS is accurate for  $\rho \gg \bar{\rho} + \Gamma$ . In the crossover region,  $\bar{\rho} - \Gamma \lesssim \rho \lesssim \bar{\rho} + \Gamma$ , both hadrons and quarks are strongly interacting, so that neither pure hadronic EOS nor pure quark EOS are reliable. Under this situation, we make a smooth interpolation of the two descriptions phenomenologically with a procedure similar to the one at high temperature (Asakawa et al. (1997)):

$$P = P_H \times f_- + P_Q \times f_+, \quad (3)$$

$$f_{\pm} = \frac{1}{2} \left( 1 \pm \tanh \left( \frac{\rho - \bar{\rho}}{\Gamma} \right) \right), \quad (4)$$

where  $P_H$  and  $P_Q$  are the pressure in the pure hadron matter and that in the pure quark matter, respectively. One should not confuse our interpolated pressure in Eq.(3) with that of the hadron-quark mixed phase associated with the first order phase transition: In our crossover picture, we are free from the ‘phase equilibrium condition’ such as  $P_Q = P_H$  at fixed chemical potential. (For phenomenological attempts to interpolate H-EOS and Q-EOS within the conventional picture of first order phase transition, see e.g. Burgio et al. (2002) and references therein.)

The energy density  $\varepsilon$  as a function of  $\rho$  is obtained by integrating the thermodynamical relation,  $P = \rho^2 \partial(\varepsilon/\rho)/\partial\rho$ , which guarantees the thermodynamical consistency for any values of  $\bar{\rho}$  and  $\Gamma$ . To explore the relation between the interpolated EOS and the maximum mass of neutron stars, we change the parameters  $(\bar{\rho}, \Gamma)$  under two conditions: (i) The system is always thermodynamically stable  $dP/d\rho > 0$ , and (ii) the normal nuclear matter is described dominantly by  $P_H$ , i.e. the condition  $\bar{\rho} - 2\Gamma > \rho_0$ .

Shown in Fig. 2 is the pressure  $P$  as a function of baryon density  $\rho$  obtained by interpolating TNI3u H-EOS (the dashed line) and NJL Q-EOS (the dash-dotted line) with  $g_v = G_S$  according to the procedure in Eq.(4). (Adopting TNI2u instead of TNI3u gives essentially the same final result.) As indicated by the shaded region on

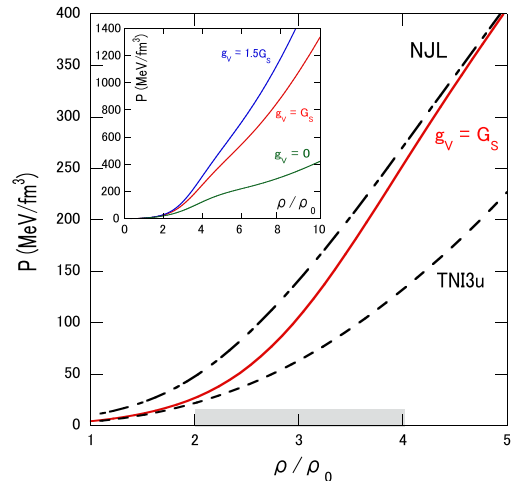


FIG. 2.— Solid line: Pressure ( $P$ ) as a function of baryon density  $\rho$  obtained by interpolating H-EOS and Q-EOS with  $g_v = G_S$  in the crossover region (the shaded region in density). Dash-dotted line: Q-EOS in the NJL model with  $g_v = G_S$ . Dashed line: H-EOS with the TNI3u interaction. The inset shows EOSs interpolated with  $g_v/G_S = 0, 1.0, 1.5$ .

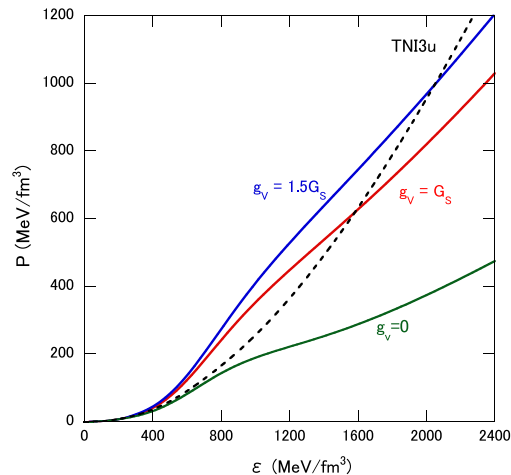


FIG. 3.— Solid lines:  $P$  vs. energy-density ( $\varepsilon$ ) for the interpolated EOSs with  $g_v/G_S = 0, 1.0, 1.5$ . Dashed line denotes hadronic matter with TNI3u interaction.

the horizontal axis, crossover parameters in this figure are  $(\bar{\rho}, \Gamma) = (3\rho_0, \rho_0)$ , which leads to a smooth interpolation between the relatively soft H-EOS and the relatively stiff Q-EOS. Note that we have  $P_H < P < P_Q$  in the crossover region, which will never be realized in the standard Maxwell or Gibbs construction assuming the first-order transition, where  $P < P_H$  always holds in the mixed phase. As will see later, the stiff EOS at  $(2-4)\rho_0$  is most important in obtaining NSs with mass greater than  $2M_\odot$ .

In the inset of Fig. 2, we show EOSs interpolated in the same crossover region but with different values of the vector coupling ( $g_v/G_S = 0, 1.0, 1.5$  motivated by Eq.(2)). As  $g_v$  increases, EOS becomes stiffer at high density, while the density where the strange-quark starts to appear ( $\rho \simeq 4\rho_0$ ) is insensitive to  $g_v$ .

In Fig. 3, we plot the pressure  $P$  as a function of the energy density  $\varepsilon$  for the three EOSs interpolated in the crossover region,  $(\bar{\rho}, \Gamma) = (3\rho_0, \rho_0)$ . These curves are the basic inputs when we solve the Tolman-Oppenheimer-

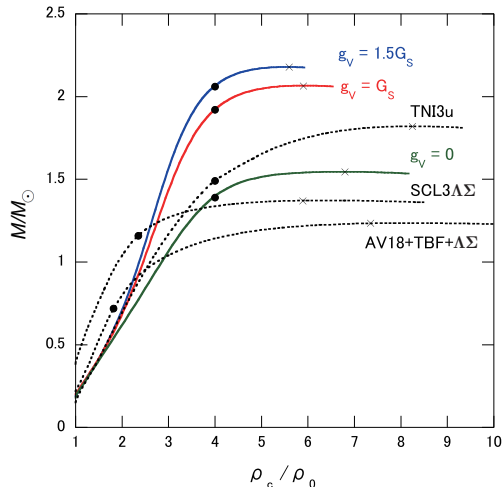


FIG. 4.— Solid lines: NS mass ( $M$ ) vs. the central baryon density ( $\rho_c$ ) obtained from interpolated EOSs between TNI3u H-EOS and NJL Q-EOS with  $g_v/G_S = 0, 1.0, 1.5$ . Dashed lines: The same quantities for H-EOS with TNI3u, AV18+TBF+ $\Lambda\Sigma$  and SCL3 $\Lambda\Sigma$ . The cross symbols denote the points of  $M_{\max}$ , while the filled circles denote the points beyond which the strangeness appears.

Volkov (TOV) equation. The case for H-EOS with TNI3u is also plotted by the dashed line for comparison. Existence of the region where  $P$  (the solid line) becomes larger than  $P_H$  (the dashed line) is essential for having large  $M_{\max}$  as shown below.

#### 5. HYBRID STAR STRUCTURE

In Fig. 4, the solid lines indicate NS masses as a function of the central density  $\rho_c$  obtained by solving the TOV equation with the EOSs given in the inset of Fig. 2, i.e., interpolated EOSs between TNI3u H-EOS and NJL Q-EOS with  $g_v/G_S = 0, 1.0, 1.5$ . Results with the hadronic EOS only (TNI3u, AV18+TBF+ $\Lambda\Sigma$  and SCL3 $\Lambda\Sigma$ ) are also plotted for comparison by the dashed lines. The filled circle indicates a point beyond which the strangeness appears in the central core of the star. The cross symbols indicate the points where  $M_{\max}$  is achieved.

For TNI3u H-EOS only, we have  $M_{\max} = 1.82M_\odot$ , while, for interpolated EOS with  $g_v/G_S \gtrsim 1$ , we have  $M_{\max} > 2M_\odot$ . This indicates that the existence of the quark core inside neutron stars is compatible with the observation of high-mass neutron star as long as (i) there is a smooth crossover between the hadronic phase and the quark phase, and (ii) there exists a strong quark correlations with repulsive nature inside the quark matter.

In Fig. 5, the solid lines indicate the mass( $M$ )-radius( $R$ ) relation of the NSs with the interpolated EOSs given in the inset of Fig. 2. Results with the H-EOS only (TNI3u, AV18+TBF+ $\Lambda\Sigma$  and SCL3 $\Lambda\Sigma$ ) are also plotted for comparison by the dashed lines. The gray band shows  $M = (1.97 \pm 0.04)M_\odot$  corresponding to PSR J1614-2230 (Demorest et al. (2010)). Because of the stiff EOS at high density for  $g_v/G_S \gtrsim 1$ , the radius  $R$  for  $0.5 \lesssim M/M_\odot \lesssim 2$  takes almost a constant value, 11–11.5 km (Özel et al. (2011)). Also, strangeness emerges only for massive stars with  $M \gtrsim 2M_\odot$ .

So far, we have taken  $(\bar{\rho}, \Gamma) = (3\rho_0, \rho_0)$  as characteristic parameters for the crossover region. In Table I, we

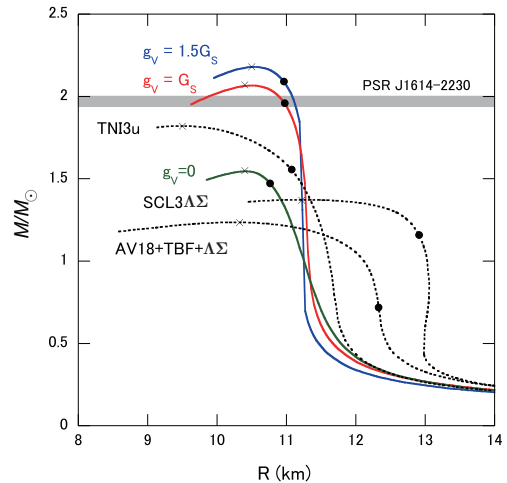


FIG. 5.— Solid lines:  $M$ - $R$  relation of the NSs with the interpolated EOSs between TNI3u H-EOS and NJL Q-EOS for  $g_v/G_S = 0, 1.0, 1.5$ . Dashed lines: The same quantities for H-EOS with TNI3u, AV18+TBF+ $\Lambda\Sigma$  and SCL3 $\Lambda\Sigma$ . The cross symbols denote the points where  $M$  reaches  $M_{\max}$ . The filled circles denote the point beyond which the strangeness appears. The gray band denotes  $M = (1.97 \pm 0.04)M_\odot$  for PSR J1614-2230 (Demorest et al. (2010).)

TABLE 1  
 $M_{\max}/M_\odot$  AND  $\rho_c/\rho_0$  IN THE PARENTHESIS UNDER THE VARIATION OF THE CROSSOVER REGION,  $\bar{\rho}$  AND  $\Gamma$ .

$\bar{\rho}$	$\Gamma/\rho_0 = 1$		$\Gamma/\rho_0 = 2$	
	$g_v = G_S$	$g_v = 1.5G_S$	$g_v = G_S$	$g_v = 1.5G_S$
$3\rho_0$	2.07 (5.9)	2.18 (5.6)	—	—
$4\rho_0$	1.93 (6.7)	2.00 (6.6)	—	—
$5\rho_0$	1.79 (7.7)	1.83 (7.4)	1.82 (7.4)	1.86 (7.3)
$6\rho_0$	1.70 (8.3)	1.70 (8.3)	1.73 (8.0)	1.74 (8.0)

show how  $M_{\max}$  and  $\rho_c$  depend on the choice of these parameters for fixed values of  $g_v$ . As the crossover region becomes lower and/or wider in baryon density, the EOS characteristic to the NS core ( $\rho = (2 - 4)\rho_0$ ) becomes stiffer. This is why  $M_{\max} > 2M_\odot$  becomes possible for  $\bar{\rho}/\rho_0 = 3$  and 4.

TABLE 2  
 $M_{\max}/M_\odot$  AND  $\rho_c/\rho_0$  IN THE PARENTHESIS FOR DIFFERENT H-EOSs WITH  $\bar{\rho} = 3\rho_0$  AND  $\Gamma/\rho_0 = 1$ .

H-EOS	$\Gamma/\rho_0 = 1$		
	$g_v = 0$	$g_v = G_S$	$g_v = 1.5G_S$
TNI3u	1.55 (6.8)	2.07 (5.9)	2.18 (5.6)
TNI2u	1.50 (7.4)	2.05 (6.1)	2.17 (5.5)
TNI3	1.51 (6.8)	2.04 (6.1)	2.16 (5.5)
AV <sub>18</sub> +TBF+ $\Lambda\Sigma$	1.52 (6.8)	2.06 (6.1)	2.17 (5.5)
SCL3 $\Lambda\Sigma$	1.55 (6.8)	2.06 (5.9)	2.17 (5.5)

Now, we examine how  $M_{\max}$  depends on the different choice of H-EOS. Shown in Table 2 is the maximum and central density for different H-EOSs with  $\bar{\rho} = 3\rho_0$  and  $\Gamma/\rho_0 = 1$ . As long as  $M_{\max}$  is concerned, the result is insensitive to the choice of the hadronic equation of state with hyperons.

## 6. SUMMARY AND CONCLUDING REMARKS

In this paper, we have investigated the maximum mass of hybrid stars with the EOS constructed on the basis of the idea of hadron-quark crossover; hadronic EOS (with hyperons and universal three-baryon repulsion) and the quark EOS (with strangeness and universal two-quark repulsion) are interpolated to model the crossover region.

We have found that massive hybrid stars compatible with  $M > 2M_{\odot}$  are possible as long as the crossover proceeds through relatively low density region, e.g.,  $\bar{\rho} = (3 - 4)\rho_0$  with  $\Gamma = \rho_0$ , and, at the same time, the quark matter is strongly interacting  $g_v/G_S \sim 1 - 1.5$ . By increasing  $g_v$  further, one can even obtain  $M_{\max}$  close to  $2.4 M_{\odot}$ . This conclusion is in remarkable contrast with the conventional EOS for hybrid star derived through the Maxwell or Gibbs construction where the resultant EOS becomes always softer than hadronic EOS and thereby leads to smaller  $M_{\max}$ .

Although we have mainly focused on the results using TNI3u H-EOS corresponding to  $\kappa = 300\text{MeV}$ , very similar results are obtained for TNI2u as shown in Table 2. This means an interesting possibility that we can reconcile the existence of massive neutron stars ( $M > 2M_{\odot}$ ) with the experimental nuclear incompressibility  $\kappa = (240 \pm 20)\text{MeV}$  (Shlomo et al. (2006)). We note that TNI3, AV18+TBF+ $\Lambda\Sigma$  and SCL3 $\Lambda\Sigma$  give almost the same  $M_{\max}$  with that of TNI3u and TNI2u. This does not, however, imply the irrelevance of the universal three-body force: For example, the interpolated EOS with H-EOS (TNI3u) and Q-EOS ( $g_v = G_s$ ) leads to strangeness mixing only above  $4\rho_0$  due to the universal three-body

force, so that the hybrid stars lighter than  $1.92M_{\odot}$  do not have strangeness (see Fig.4). Then, the hyperon direct Urca process (e.g.,  $\Lambda \rightarrow p + e^{-} + \bar{\nu}_e$ ,  $p + e^{-} \rightarrow \Lambda + \nu_e$ ), which leads to extremely rapid neutrino-cooling and contradicts observations (Takatsuka et al. (2006)), does not take place except for massive NSs.

Our massive hybrid stars with  $M > 2M_{\odot}$  originate from the transition from the soft EOS to stiff EOS in the density region  $\rho \sim (2 - 4)\rho_0$  due to the hadron-quark crossover. Therefore it would be important to explore such crossover by independent laboratory experiments with medium-energy heavy-ion collisions.

Finally, we remark that the crossover region may have rich non-perturbative phases such as color superconducting phases, inhomogeneous phases, the quarkyonic phase and so on (Fukushima et al. (2011)). How these structures affect the basic conclusion of the present paper would be an interesting future problem to be examined.

K.M. and T.H. thank Wolfram Weise for discussions. T.T. thanks Ryoza Tamagaki, Toshitaka Tatsumi and Shigeru Nishizaki for discussions and interests in this work. We also thank K. Tsubakihara and A. Ohnishi for providing us with the numerical data of the SCL3 EOS. This research was supported in part by MEXT Grant-in-Aid for Scientific Research on Innovative Areas(No.2004:20105003) by JSPS Grant-in-Aid for Scientific Research (B) No.22340052, and by RIKEN 2012 Strategic Programs for R & D.

## REFERENCES

- Akmal, A., Pandharipande, V.R. & Ravenhall, D.G. 1998, Phys. Rev. C58, 1804
- Asakawa, M., & Yazaki, K. 1989, Nucl. Phys. A504, 668
- Asakawa, M., & Hatsuda, T. 1997, Phys. Rev. D55, 4488
- Baldo, M., Burgio, & G.F. Schulze, H.J. 2000, Phys. Rev. C61, 055801
- Baym, G. 1979, Physica 96A, 131
- Baym, G., Hatsuda, T., Tachibana, M. & Yamamoto, N. 2008, J. Phys. G G35, 104021
- Bonanno, L., & Sedrakian, A. 2012, Astron. Astrophys. 539, A16
- Bratovic, N., Hatsuda, T., & Weise, W. 2012, arXiv:1204.3788 [hep-ph]
- Buballa, M. 2005, Phys. Rept. 407, 205.
- Burgio, G. F., Baldo, M., Sahu, P. K. & Schulze, H. J. 2002, Phys. Rev. C66, 025802.
- Celik, T., Karsch, F., & Satz, H. 1980, Phys. Lett. B97, 128.
- Chen, H., Baldo, M. Burgio, G. F. & Schulze, H.-J. 2012, arXiv:1203.0158 [nucl-th]
- Demorest, P.B., Pennucci, T., Ranson, S.M., Roberts, M.S.E., & Hessels, J.W.T. 2010, Nature 467, 1081
- Friedman, B. & Pandharipande, V.R. 1981, Nucl. Phys. A361, 502
- Fukushima, K. & Hatsuda, T. 2011, Rept. Prog. Phys. 74, 014001
- Hatsuda, T., & Kunihiro, T. 1994, Phys. Rep., 247, 221
- Kim, K., Lee, H. K., & Rho, M. 2011, Phys. Rev. C84, 035810
- Klahn, T., Blaschke, D. & Lastowiecki, R. 2011, arXiv:1111.6889 [nucl-th]
- Klevansky, S.P. 1992, Rev. Mod. Phys. 64, 649 1992
- Kurkela, A., Romatschke, P., Vuorinen, A., & Wu, B. 2010 arXiv 1006.4062 [astro-ph.HE]
- Lattimer, J. M., & Prakash, M. 2010, arXiv 1012.3208 [astro-ph.SR]
- Lourenco, O., Dutra, M., Frederico, T., Delfino, A., & Malheiro, M. 2012, Phys. Rev. D85, 097504
- Maeda, K., Baym, G., & Hatsuda, T. 2009, Phys. Rev. Lett. 103, 085301
- Nishizaki, S., Yamamoto, Y., & Takatsuka, T. 2001, Prog. Theor. Phys. 105, 607
- Nishizaki, S., Yamamoto, Y., & Takatsuka, T. 2002, Prog. Theor. Phys. 108, 703
- Özel, F., Psaltis, D., Ransom, S., Demorest, P., & Alford, M. 2010, ApJ, 724, L199
- Özel, F., Gould, A. & Guver, T. 2012, ApJ, 748, 5
- Schramm, S., Dexheimer, V., Negreiros, R., Schurhoff, T., & Steinheimer, J. 2012, arXiv 1202.5113 [astro-ph.SR]
- Shlomo, S., Kolomietz, V.M. & Colò, G. 2006, Eur. Phys. J. A30, 23
- Takatsuka, T., Nishizaki, S., Yamamoto, Y. & Tamagaki, R. 2006, Prog. Theor. Phys. 115, 355
- Takatsuka, T., Nishizaki, S., & Tamagaki, R. 2008 Proc. Int. Symp. "FM50" (AIP Conference proceedings) 209
- Takatsuka, T., Hatsuda, T., & Masuda, K. 2011, Proceedings of the 11th Int. Symp. on "Origin of Matter and Evolution of Galaxies (OMEG 11)" (Nov.14-17, 2011, RIKEN, Wako, Japan)
- Tsubakihara, K., Maekawa, H., Matsumiya, H. & Ohnishi, A. 2010, Phys. Rev. C81, 065206
- Vogl, U., & Weise, W. 1991, Prog. Part. Nucl. Phys. 27, 195
- Weissenborn, S., Sagert, I., Pagliara, G., Hempel, M., & Schaeffner-Bielich, J. 2011, ApJ, 740, L14
- Whittenbury, D. L., Carroll, J.D., Thomas, A. W., Tsushima, K. & Stone, J.R. 2012, arXiv:1204.2614 [nucl-th]